5

The Ekman Layer

Summary: Frictional forces, neglected in the previous chapter, are now investigated. Their main effect is to create horizontal boundary layers that support a flow transverse to the main flow of the fluid.

5-1 ON THE IMPORTANCE OF FRICTION

After the development of the equations governing geophysical motions (Sections 3-1 through 3-5), a scale analysis was performed to evaluate the relative importance of the various terms (Section 3-6). In the horizontal momentum equations [(3-25) and (3-26)], each term was compared to the Coriolis term, and a corresponding dimensionless ratio was defined. For vertical friction, the dimensionless ratio was the Ekman number:

$$Ek = \frac{\nu}{\Omega H^2}, \tag{5-1}$$

where ν is the kinematic viscosity, Ω is the ambient rotation rate, and H is the depth scale of the motion (the total depth if the fluid is homogeneous).

Typical geophysical flows, as well as laboratory experiments, yield very small

Ekman numbers. For example, in the ocean at midlatitudes ($\Omega \simeq 10^{-4}$ s^{-1}), motions modeled with an eddy-intensified viscosity $\nu = 10^{-2}$ m^2/s (much larger than the nominal molecular viscosity of water, which is equal to 1.0×10^{-6} m^2/s) and extending over a depth of about 1000 m are characterized by an Ekman number of about 10^{-4}.

The smallness of the Ekman number indicates that vertical friction plays a very minor role in the balance of forces and may, consequently, be omitted. This is usually done and with great success. However, something is then lost. The frictional terms happen to be those with the highest order of derivatives among all terms of the momentum equations. Thus, when friction is neglected, the order of the set of differential equations is reduced, and not all boundary conditions can be applied simultaneously. Usually, slipping along the bottom must be accepted.

Since Ludwig Prandtl and his general theory of boundary layers, we know that in such a circumstance the fluid system exhibits two distinct behaviors: At some distance from the boundaries, in what is called the *interior*, friction is usually negligible, whereas, near a boundary (wall) and across a short distance, called the *boundary layer*, friction acts to bring the finite interior velocity to zero at the wall.

The depth, d, of this thin layer is such that the Ekman number is on the order of one at that scale:

$$\frac{\nu}{\Omega d^2} \sim 1,$$

which leads to

$$d \sim \sqrt{\frac{\nu}{\Omega}}. \tag{5-2}$$

Obviously, d is much less than H, and the boundary layer occupies a very small portion of the flow domain. For the oceanic values cited above ($\nu = 10^{-2}$ m^2/s and $\Omega = 10^{-4}$ s^{-1}), d is 10 m.

Because of the Coriolis effect, the frictional boundary layer of geophysical flows, called the *Ekman layer*, differs greatly from the boundary layer in nonrotating fluids. Although, the traditional boundary layer has no particular thickness and grows either downstream or with time, the existence of the depth scale, d, in rotating fluids suggests that the Ekman layer can be characterized by a fixed thickness. [Note that as the rotational effects disappear ($\Omega \to 0$), d tends to infinity, exemplifying this essential difference between rotating and nonrotating fluids.]

5-2 THE BOTTOM EKMAN LAYER

Let us consider a uniform, geostrophic flow in a homogeneous fluid over a flat bottom (Figure 5-1). This bottom exerts a frictional stress against the flow, bringing the velocity gradually to zero within a thin layer above the bottom. We now solve for the structure of this layer.

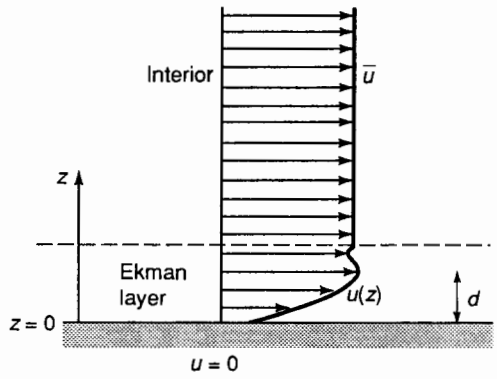

Figure 5-1 Frictional influence of a flat bottom on a uniform flow.

In the absence of horizontal gradients (the interior flow is said to be uniform) and of temporal variations, the continuity equation, (3-28), yields $\partial w/\partial z = 0$ and thus $w = 0$ in the thin layer near the bottom. The remaining equations are the following reduced forms of (3-25) through (3-27):

$$-fv = -\frac{1}{\rho_0}\frac{\partial p}{\partial x} + \nu\frac{\partial^2 u}{\partial z^2} \tag{5-3}$$

$$+fu = -\frac{1}{\rho_0}\frac{\partial p}{\partial y} + \nu\frac{\partial^2 v}{\partial z^2} \tag{5-4}$$

$$0 = -\frac{1}{\rho_0}\frac{\partial p}{\partial z}, \tag{5-5}$$

where f is the Coriolis parameter (taken as a constant here), ρ_0 is the fluid density, and ν is the kinematic viscosity. The horizontal gradient of the pressure p is retained because a uniform flow requires a uniformly varying pressure (Section 4-1). Let us align the x-axis with the direction of the interior flow, which is of velocity $\bar{u}$. The boundary conditions are then

Bottom $(z = 0)$: $\quad u = 0, \quad v = 0,$ (5-6)

Toward the interior $(z \to \infty)$: $\quad u = \bar{u}, \quad v = 0, \quad p = \bar{p}(x,y).$ (5-7)

By virtue of equation (5-5), the dynamic pressure p is the same at all depths; thus, $p = \bar{p}(x, y)$ in the outer flow as well as throughout the boundary layer. In the outer flow $(z \to \infty)$, equations (5-3) and (5-4) relate the velocity to the pressure gradient:

$$0 = -\frac{1}{\rho_0}\frac{\partial \bar{p}}{\partial x},$$

$$f\bar{u} = -\frac{1}{\rho_0}\frac{\partial \bar{p}}{\partial y} = \text{constant}.$$

Substitution of these derivatives in the same equations, which are now taken at any depth, yields

$$-fv = \nu \frac{d^2u}{dz^2}$$

$$f\,(u - \overline{u}) = \nu \frac{d^2v}{dz^2}.$$

Seeking a solution of the type $u = \overline{u} + A \exp(\lambda z)$ and $v = B \exp(\lambda z)$, we find that λ obeys $\nu^2\lambda^4 + f^2 = 0$; that is,

$$\lambda = \pm (1 \pm i) \frac{1}{d}$$

where the distance d is defined by

$$d = \sqrt{\frac{2\nu}{f}}. \tag{5-8}$$

Here, we have restricted ourselves to cases with positive f (Northern Hemisphere). Note the similarity to (5-2). Boundary conditions (5-7) rule out the exponentially growing solutions, leaving

$$u = \overline{u} + e^{-z/d}\left(A \cos \frac{z}{d} + B \sin \frac{z}{d}\right)$$

$$v = e^{-z/d}\left(B \cos \frac{z}{d} - A \sin \frac{z}{d}\right),$$

and the application of the remaining boundary conditions (5-6) yields $A = -\overline{u}$, $B = 0$, or

$$u = \overline{u}\left(1 - e^{-z/d} \cos \frac{z}{d}\right) \tag{5-9}$$

$$v = \overline{u}\, e^{-z/d} \sin \frac{z}{d}. \tag{5-10}$$

This solution has a number of important properties. First and foremost, we notice that the distance over which it approaches the interior solution is on the order of d. Thus, expression (5-8) gives the thickness of the boundary layer. For this reason, d is called the *Ekman depth*. A comparison with (5-2) confirms the earlier argument that the boundary-layer thickness is the one corresponding to a local Ekman number near unity.

The preceding solution also tells us that there is, in the boundary layer, a flow transverse to the interior flow ($v \neq 0$). Very near the bottom ($z \to 0$), this component is equal to the downstream velocity ($u \sim v \sim \overline{u}z/d$), thus implying that the velocity there is at 45 degrees to the left of the interior velocity (Figure 5-2). (The boundary flow is to the right of the interior flow for $f < 0$.) Farther up, where u reaches a first

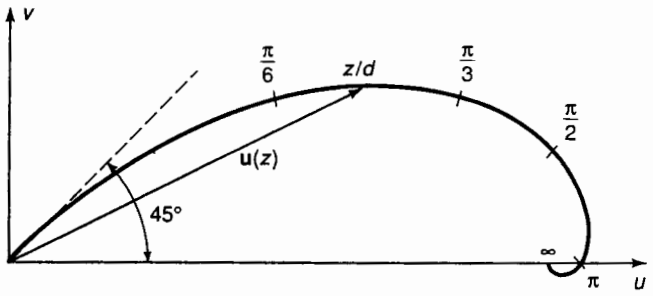

Figure 5-2 The velocity spiral in the bottom Ekman layer. The figure is drawn for the Northern Hemisphere ($f > 0$), and the deflection is to the left of the current above the layer. The reverse holds for the Southern Hemisphere.

maximum ($z = 3\pi d/4$), the velocity in the direction of the flow is greater than in the interior ($u = 1.07\bar{u}$). (Viscosity can sometimes fool us!)

It is instructive to calculate the net transport of fluid transverse to the main flow:

$$V = \int_0^\infty v \, dz = \frac{\bar{u}d}{2}, \tag{5-11}$$

which is proportional to the interior velocity and the Ekman depth.

5-3 GENERALIZATION TO NONUNIFORM CURRENTS

Let us now consider a more complex interior flow, namely, a spatially nonuniform flow that is varying on a scale sufficiently large to be in geostrophic equilibrium (low Rossby number, as in Section 4-1). Thus,

$$-f\bar{v} = -\frac{1}{\rho_0}\frac{\partial \bar{p}}{\partial x}, \qquad f\bar{u} = -\frac{1}{\rho_0}\frac{\partial \bar{p}}{\partial y},$$

where the pressure $\bar{p}(x, y, t)$ is arbitrary. For a constant Coriolis parameter, this flow is nondivergent ($\partial\bar{u}/\partial x + \partial\bar{v}/\partial y = 0$). The boundary-layer equations are now

$$-f(v - \bar{v}) = \nu \frac{\partial^2 u}{\partial z^2}, \qquad f(u - \bar{u}) = \nu \frac{\partial^2 v}{\partial z^2}, \tag{5-12a,b}$$

and the solution is

$$u = \bar{u}\left(1 - e^{-z/d}\cos\frac{z}{d}\right) - \bar{v}\, e^{-z/d}\sin\frac{z}{d} \tag{5-13a}$$

$$v = \bar{u}\, e^{-z/d}\sin\frac{z}{d} + \bar{v}\left(1 - e^{-z/d}\cos\frac{z}{d}\right). \tag{5-13b}$$

The transport attributed to the boundary-layer structure has components given by

$$U = \int_0^\infty (u - \bar{u})\, dz = -\frac{d}{2}(\bar{u} + \bar{v}) \tag{5-14a}$$

$$V = \int_0^\infty (v - \overline{v})\, dz = \frac{d}{2}(\overline{u} - \overline{v}). \tag{5-14b}$$

Since this transport is not necessarily parallel to the interior flow, it is likely to have a nonzero divergence. Indeed,

$$\frac{\partial U}{\partial x} + \frac{\partial V}{\partial y} = \int_0^\infty \left(\frac{\partial u}{\partial x} + \frac{\partial v}{\partial y}\right) dz = -\frac{d}{2}\left(\frac{\partial \overline{v}}{\partial x} - \frac{\partial \overline{u}}{\partial y}\right) = -\frac{d}{2\rho_0 f}\nabla^2 \overline{p}. \tag{5-15}$$

The flow in the boundary layer converges or diverges if the interior flow has a relative vorticity. The situation is depicted in Figure 5-3. The question is: From where

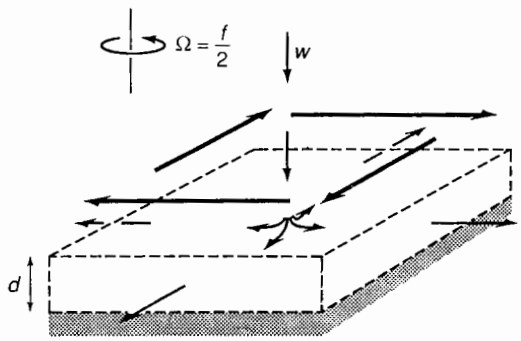

Figure 5-3 Divergence in the bottom Ekman layer and compensating downwelling in the interior. Such situation arises in the presence of an anticyclonic gyre in the interior. Similarly, interior cyclonic motion causes convergence in the bottom Ekman layer and upwelling in the interior.

is the fluid coming or where it is going to meet such convergence or divergence? Because of the presence of a solid bottom, the only possibility is that it be supplied from the interior by means of a vertical velocity. But, remember (Section 4-1) that geostrophic flows must be characterized by

$$\frac{\partial \overline{w}}{\partial z} = 0;$$

that is, the vertical velocity must occur throughout the depth of the fluid. Of course, since the divergence of the flow in the Ekman layer is proportional to the Ekman depth, d, which is very small, this vertical velocity is very weak.

The vertical velocity in the interior, called *Ekman pumping*, can be evaluated by a vertical integration of the continuity equation (3-28), using $w(z = 0) = 0$ and $w(z \to \infty) = \overline{w}$:

$$\overline{w} = -\int_0^\infty \left(\frac{\partial u}{\partial x} + \frac{\partial v}{\partial y}\right) dz = \frac{d}{2}\left(\frac{\partial \overline{v}}{\partial x} - \frac{\partial \overline{u}}{\partial y}\right) = \frac{d}{2\rho_0 f}\nabla^2 \overline{p}. \tag{5-16}$$

So, the greater the vorticity of the mean flow, the greater the upwelling/downwelling. Also, the effect increases toward the equator (decreasing $f = 2\Omega \sin \varphi$ and increasing d).

5-4 THE SURFACE EKMAN LAYER

An Ekman layer occurs not only along bottom surfaces but wherever there is a horizontal frictional stress. This is the case, for example, along the ocean surface, where waters are subject to a wind stress. In fact, this is precisely the situation first examined by Vagn Walfrid Ekman (see the biography at the end of this chapter). Fridjof Nansen, a Norwegian oceanographer, had noticed during his cruises to northern latitudes that icebergs drift not downwind but systematically at some angle to the right of the wind. Ekman, his student at the time, reasoned that the cause of this bias was the earth's rotation and subsequently developed the boundary-layer model that now bears his name. The solution was originally published in his 1902 doctoral thesis and again, in a more complete article, three years later (Ekman, 1905). In a subsequent article (Ekman, 1906), he mentioned the relevance of his theory to the atmosphere, with the wind approaching the geostrophic wind with height.

Let us consider the situation depicted in Figure 5-4, where an ocean region with interior flow field $(\overline{u}, \overline{v})$ is subjected to a wind stress (τ^x, τ^y) along its surface. Again,

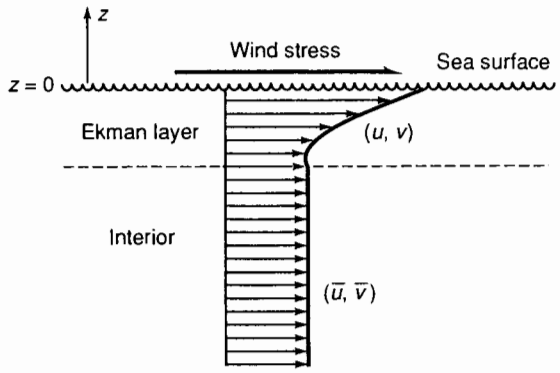

Figure 5-4 The surface Ekman layer generated by a wind stress on the ocean.

assuming steady conditions, a homogeneous fluid, and a geostrophic interior, we obtain the following equations and boundary conditions for the flow field (u, v) in the surface Ekman layer:

$$-f(v - \overline{v}) = \nu \frac{\partial^2 u}{\partial z^2} \tag{5-17a}$$

$$+f(u - \overline{u}) = \nu \frac{\partial^2 v}{\partial z^2}, \tag{5-17b}$$

$$\text{Surface } (z = 0): \qquad \rho_0 \nu \frac{\partial u}{\partial z} = \tau^x, \ \rho_0 \nu \frac{\partial v}{\partial z} = \tau^y, \tag{5-17c}$$

$$\text{Toward interior } (z \to -\infty): \ u = \overline{u}, \quad v = \overline{v}. \tag{5-17d}$$

The solution to this problem is

$$u = \bar{u} + \frac{\sqrt{2}}{\rho_0 f d}\, e^{z/d}\left[\tau^x \cos\left(\frac{z}{d} - \frac{\pi}{4}\right) - \tau^y \sin\left(\frac{z}{d} - \frac{\pi}{4}\right)\right], \tag{5-18a}$$

$$v = \bar{v} + \frac{\sqrt{2}}{\rho_0 f d}\, e^{z/d}\left[\tau^x \sin\left(\frac{z}{d} - \frac{\pi}{4}\right) + \tau^y \cos\left(\frac{z}{d} - \frac{\pi}{4}\right)\right], \tag{5-18b}$$

in which we note that the departure from the interior flow $(\bar{u}, \bar{v})$ is exclusively due to the wind stress. In other words, it does not depend on the interior flow. Moreover, this wind-driven flow component is inversely proportional to the Ekman-layer depth, d, and can be very large. Physically, if the fluid is almost inviscid (small ν, hence small d), a moderate surface stress can generate large velocities.

The wind-driven horizontal transport in the surface Ekman layer has components given by

$$U = \int_{-\infty}^{0} (u - \bar{u})\, dz = \frac{1}{\rho_0 f}\, \tau^y \tag{5-19a}$$

$$V = \int_{-\infty}^{0} (v - \bar{v})\, dz = \frac{-1}{\rho_0 f}\, \tau^x . \tag{5-19b}$$

Surprisingly, it is oriented perpendicular to the direction of the wind stress (Figure 5-5), to the right in the Northern Hemisphere and to the left in the Southern Hemisphere. This fact explains why icebergs, which have mass that is mostly underwater, systematically drift to the right of the wind in the North Atlantic.

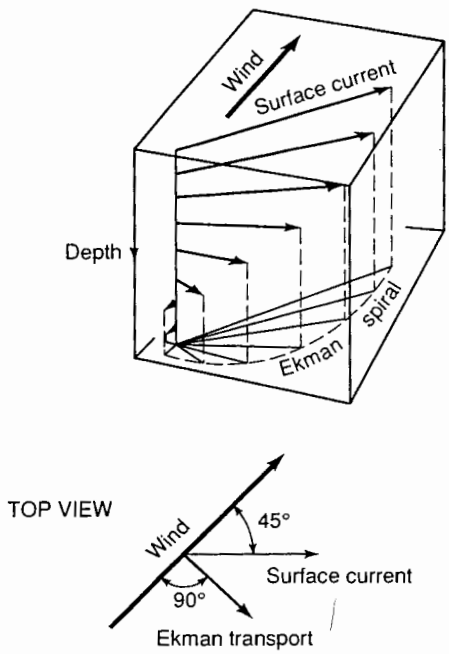

Figure 5-5 Structure of the surface Ekman layer. The figure is drawn for the Northern Hemisphere ($f > 0$), and the deflection is to the right of the surface stress. The reverse holds for the Southern Hemisphere.

In analogy with the bottom Ekman layer, let us determine the divergence of the flow, integrated over the boundary layer:

$$\int_{-\infty}^{0} \left(\frac{\partial u}{\partial x} + \frac{\partial v}{\partial y} \right) dz = \frac{1}{\rho_0 f} \left(\frac{\partial \tau^y}{\partial x} - \frac{\partial \tau^x}{\partial y} \right).$$

The contribution is entirely due to the wind stress since the interior geostrophic flow is nondivergent (for constant f). It is proportional to the wind-stress curl and, most importantly, it is independent of the value of the viscosity.

If the wind stress has a nonzero curl, the divergence of the Ekman transport must be provided by a vertical velocity throughout the interior. A vertical integration of the continuity equation, (3-28), across the Ekman layer with $w(z = 0)$ and $w(z \to -\infty) = \overline{w}$ yields

$$\overline{w} = + \int_{-\infty}^{0} \left(\frac{\partial u}{\partial z} + \frac{\partial v}{\partial z} \right) dz = \frac{1}{\rho_0 f} \left(\frac{\partial \tau^y}{\partial x} - \frac{\partial \tau^x}{\partial y} \right). \tag{5-20}$$

This vertical velocity is called *Ekman pumping*. In the Northern Hemisphere ($f > 0$), a clockwise wind pattern (negative curl) generates a downwelling (Figure 5-6a), whereas a counterclockwise wind pattern causes upwelling (Figure 5-6b). The directions are opposite in the Southern Hemisphere. Ekman pumping is a very effective mechanism by which winds drive subsurface ocean currents (see Chapter 8).

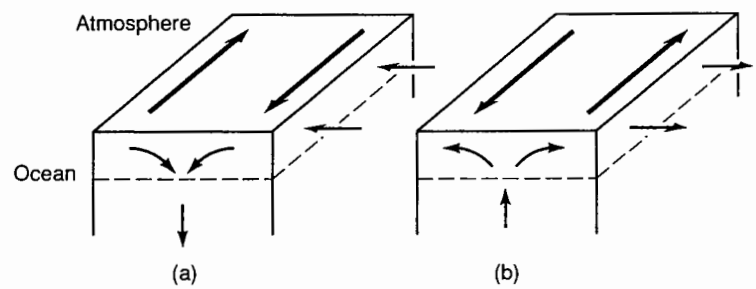

Figure 5-6 Ekman pumping in an ocean subject to sheared winds (Northern Hemisphere).

5-5 THE EKMAN LAYER OVER UNEVEN TERRAIN

Before concluding this chapter, it is noteworthy to explore how irregular topography affects the structure of the Ekman layer and, in particular, the magnitude of the vertical velocity in the interior. For this, consider a horizontal geostrophic interior flow $(\overline{u}, \overline{v})$, not necessarily spatially uniform, over an uneven terrain of elevation $z = b(x, y)$ above a horizontal reference level. To be faithful to our restriction (Section 3-4) to geophysical flows much wider than they are thick, we shall assume that the bottom slope $(\partial b/\partial x, \partial b/\partial y)$ is everywhere small ($\ll 1$). This is hardly a restriction in most atmospheric and oceanic situations.

Our governing equations are again (5-12a) and (5-12b), coupled to the continuity equation (3-28), but the boundary conditions are now

$$\text{Bottom } (z = b): \qquad u = 0,\ v = 0,\ w = 0, \tag{5-21}$$

$$\text{Toward the interior } (z \to \infty): \quad u = \overline{u},\ v = \overline{v}. \tag{5-22}$$

The solution that satisfies the interior boundary condition (5-22) is

$$u = \overline{u} + e^{-z/d}\left(A \cos \frac{z}{d} + B \sin \frac{z}{d}\right)$$

$$v = \overline{v} + e^{-z/d}\left(B \cos \frac{z}{d} - A \sin \frac{z}{d}\right),$$

where the "constants" of integration A and B are, in general, dependent on x and y. Imposing $u = v = 0$ along the bottom $(z = b)$, we determine these constants as functions of $b(x, y)$ and obtain

$$u = \overline{u} - e^{(b-z)/d}\left(\overline{u} \cos \frac{z-b}{d} + \overline{v} \sin \frac{z-b}{d}\right) \tag{5-23a}$$

$$v = \overline{v} + e^{(b-z)/d}\left(\overline{u} \sin \frac{z-b}{d} - \overline{v} \cos \frac{z-b}{d}\right). \tag{5-23b}$$

We note that the vertical thickness of the boundary layer is still measured by $d = \sqrt{2\nu/f}$. However, the boundary layer is now oblique, and its true thickness, measured perpendicular to the bottom, is reduced by the cosine of the bottom slope.

The vertical velocity is then determined from the continuity equation:

$$\frac{\partial w}{\partial z} = -\frac{\partial u}{\partial x} - \frac{\partial v}{\partial y}$$

$$= e^{(b-z)/d}\left\{\left(\frac{\partial \overline{v}}{\partial x} - \frac{\partial \overline{u}}{\partial y}\right) \sin \frac{z-b}{d}\right.$$

$$+ \frac{1}{d}\frac{\partial b}{\partial x}\left[(\overline{u} - \overline{v}) \cos \frac{z-b}{d} + (\overline{u} + \overline{v}) \sin \frac{z-b}{d}\right]$$

$$\left. + \frac{1}{d}\frac{\partial b}{\partial y}\left[(\overline{u} + \overline{v}) \cos \frac{z-b}{d} - (\overline{u} - \overline{v}) \sin \frac{z-b}{d}\right]\right\},$$

where use has been made of the fact that the interior geostrophic flow has no divergence $(\partial \overline{u}/\partial x + \partial \overline{v}/\partial y = 0)$. A vertical integration from the bottom $(z = b)$, where the vertical velocity vanishes $(w = 0)$ into the interior $(z \to +\infty)$ where the vertical velocity assumes a vertically uniform value $(w = \overline{w})$, yields

$$\overline{w} = \left(\overline{u}\frac{\partial b}{\partial x} + \overline{v}\frac{\partial b}{\partial y}\right) + \frac{d}{2}\left(\frac{\partial \overline{v}}{\partial x} - \frac{\partial \overline{u}}{\partial y}\right). \tag{5-24}$$

The interior vertical velocity thus consists of two parts: a component that ensures no normal flow to the bottom [see (4-10)] and an Ekman-pumping contribution, as if the bottom were horizontally flat [see (5-16)].

The vanishing of the flow component perpendicular to the bottom must be met by the inviscid dynamics of the interior, giving rise to the first contribution to $\overline{w}$. The role of the boundary layer is to bring the tangential velocity to zero at the bottom. This explains the second contribution to $\overline{w}$. Note that the Ekman pumping is proportional to the bottom slope.

5-6 THE EKMAN LAYER IN REAL GEOPHYSICAL FLOWS

The preceding models of bottom and surface Ekman layers are highly idealized, and we do not expect their solutions to match closely actual atmospheric and oceanic observations (except in some cases; see Figure 5-7). Two factors, among others, account for substantial differences: turbulence and stratification.

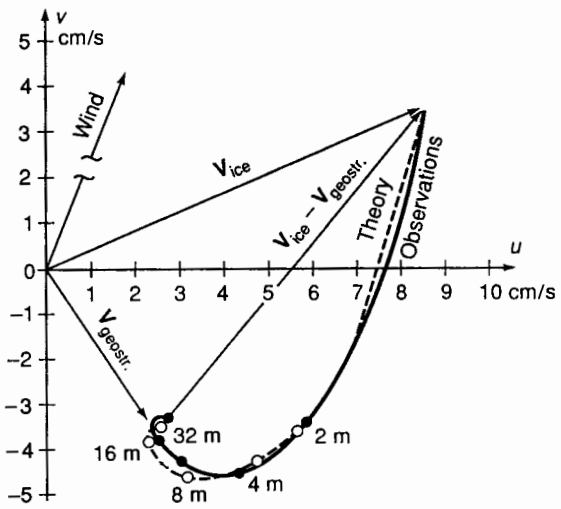

Figure 5-7 Comparison between observed currents below a drifting ice floe at 84.3°N and theoretical predictions based on an eddy viscosity $\nu = 2.4 \times 10^{-3}$ m^2/s. (Reprinted from *Deep-Sea Research*, 13, Kenneth Hunkins, Ekman drift currents in the Arctic Ocean, p. 614, copyright 1966, with kind permission from Pergamon Press Ltd, Headington Hill Hall, Oxford 0X3 0BW, UK.)

It was noted at the end of Chapter 3 that geophysical flows have large Reynolds numbers and are therefore in a state of turbulence. Replacing the molecular viscosity of the fluid by a much greater eddy viscosity is a first attempt to recognize the enhanced transfer of momentum in a turbulent flow. However, in a shear flow such as in an Ekman layer, the turbulence is not homogeneous, being more vigorous where the shear is greater and also partially suppressed in the proximity of the boundary where the size of turbulent eddies is restricted. In the absence of an exact theory of turbulence, several schemes can be proposed; and, as a minimum, the eddy viscosity should be made to vary in the vertical (Madsen, 1977). A number of models have been proposed (for a

review, see Mellor and Yamada, 1982), with varying degrees of success. Despite numerous disagreements among models and with field observations, two results nonetheless stand out as quite general. The first is that the angle between the near-boundary velocity and that in the interior or that of the surface stress (depending on the type of Ekman layer) is systematically found to be substantially less than the theoretical value of 45° and to range between 5° and 20°. The second result is a formula for the vertical scale of the Ekman-layer thickness:

$$d \simeq 0.4 \frac{u_*}{f}, \tag{5-25}$$

where u_* is the turbulent friction velocity traditionally defined from the magnitude $\tau = (\tau^{x2} + \tau^{y2})^{1/2}$ of the stress along the boundary by

$$u_* = \sqrt{\frac{\tau}{\rho_0}}. \tag{5-26}$$

This result can be briefly explained as follows. In turbulence (Tennekes and Lumley, 1972), the eddy viscosity is proportional to the product of a turbulent velocity and a mixing length, characteristic of the local turbulent activity. Taking u_* as the turbulent velocity and the (unknown) Ekman-layer depth scale, d, as the size of the largest turbulent eddies, we write

$$\nu \sim u_* d. \tag{5-27}$$

Then, using rule (5-2) to determine the layer thickness, we obtain

$$1 \sim \frac{\nu}{fd^2} \sim \frac{u_*}{fd},$$

which immediately leads to (5-25). The numerical factor in (5-25) has been derived empirically. Whereas 0.4 is the most commonly accepted value, there is evidence that certain oceanic conditions call for a somewhat smaller value (Mofjeld and Lavelle, 1984; Stigebrandt, 1985).

The other major element missing from the Ekman-layer models of the previous sections is the presence of vertical density stratification. Although the effects of stratification is not discussed in detail until Chapter 9, it can be anticipated here that the gradual change of density with height (lighter fluid above heavier fluid) hinders vertical movements, thereby reducing vertical mixing of momentum by turbulence; it also allows the motions at separate levels to act less coherently. As a consequence, stratification reduces the thickness of the Ekman layer and increases the veering of the velocity vector with height.

The surface atmospheric layer during daytime over land and above warm currents at sea is frequently in a state of convection because of heating from below. In such situations, the Ekman dynamics give way to convective motions, and a controlling factor, besides the geostrophic wind aloft, is the intensity of the surface heat flux. An elementary model is presented later (Section 11-4). Because Ekman dynamics then play

a secondary role, the layer is simply called the *atmospheric boundary layer*. The interested reader is referred to the book by Sorbjan (1989).

PROBLEMS

5-1. It is well known that the fragments of tea leaves at the bottom of a stirred cup of tea conglomerate toward the center. Explain this phenomenon with Ekman-layer dynamics. Also explain why the tea leaves go to the center irrespective of the direction of stirring (clockwise or counterclockwise).

5-2. Assume that the atmospheric Ekman layer over the earth's surface at latitude 45°N can be modeled with a turbulent kinematic viscosity $\nu = 10\ \text{m}^2/\text{s}$. If the geostrophic velocity above the layer is 10 m/s and is uniform, what is the vertically integrated flow across the isobars (pressure contours)? Is there any vertical velocity?

5-3. Meteorological observations above New York City (41°N) reveal a neutral atmospheric boundary layer (no convection and no stratification) and a westerly geostrophic wind of 12 m/s at 1000 m above street level. Under neutral conditions, Ekman-layer dynamics apply. Using an eddy viscosity of $10\ \text{m}^2/\text{s}$, determine the wind speed and direction atop the World Trade Center (height: 411 m).

5-4. Using data from the Problem 5-3 and estimating the wind force per unit height and the direction of the wind to be $F = 0.93\rho L V^2$, where $\rho = 1.20\ \text{kg/m}^3$ is the standard air density, $L = 50$ m is the building width, and $V(z) = (u^2 + v^2)^{1/2}$ is the wind speed at the height considered, determine the net normal force on the tower of the World Trade Center facing west.

5-5. You are working for a company that plans to deposit high-level radioactive wastes on the bottom of the ocean, at a depth of 3000 m. This site (latitude: 33°N) is known to be at the center of a permanent counterclockwise vortex. Locally, the vortex flow can be assimilated to a solid-body rotation with angular speed equal to $10^{-5}\ \text{s}^{-1}$. Assuming a homogeneous ocean and a steady, geostrophic flow, estimate the upwelling rate at the vortex center. How many years will it take for the radioactive wastes to arrive at the surface? Take $f = 8 \times 10^{-5}\ \text{s}^{-1}$ and $\nu = 10^{-2}\ \text{m}^2/\text{s}$.

5-6. Between 15°N and 45°N, the winds over the North Pacific consist mostly of the easterly trades (15°N to 30°N) and the westerlies (30°N to 45°N). An adequate representation is

$$\tau^x = \tau_0 \sin\left(\frac{\pi y}{2L}\right), \qquad \tau^y = 0, \qquad -L \le y \le L,$$

where $\tau_0 = 0.15\ \text{N/m}^2$ is the maximum wind stress and $L = 1670$ km. Taking $\rho_0 = 1028\ \text{kg/m}^3$ and the value of the Coriolis parameter corresponding to 30°N, calculate the Ekman pumping. Which way is it directed? Calculate the vertical volume flux over the entire 15°−45°N strip of the North Pacific (width = 8700 km). Express your answer in sverdrup units (1 sverdrup = 1 Sv = $10^6\ \text{m}^3/\text{s}$).

5-7. Approximating the variation of the Coriolis parameter with latitude by writing $f = f_0 + \beta_0 y$, where y is the northward coordinate (beta-plane approximation; see Section 6-4), show that the vertical velocity below the surface Ekman layer of the ocean is given by

$$\overline{w}(z) = \frac{1}{\rho_0}\left[\frac{\partial}{\partial x}\left(\frac{\tau^y}{f}\right) - \frac{\partial}{\partial y}\left(\frac{\tau^x}{f}\right)\right] - \frac{\beta_0}{f}\int_z^0 \overline{v}\, dz, \qquad (5\text{-}28)$$

where τ^x and τ^y are the zonal and meridional wind-stress components, respectively, and $\overline{v}$ is the meridional velocity in the geostrophic interior below the Ekman layer.

5-8. Determine the vertical distribution of horizontal velocity in a 3-m-thick water layer floating above a seawater (density = 1020 kg/m^3) current flowing eastward at 20 cm/s and subject to a northerly wind stress of 0.2 N/m^2. Take $f = 10^{-4}$ s^{-1} and $\nu = 10^{-2}$ m^2/s. In which direction is the net transport in this brackish layer?

5-9. Redo Problem 5-8 with $f = 0$ and compare the two solutions. What can you conclude about the role of the Coriolis force in this case?

SUGGESTED LABORATORY DEMONSTRATION

Equipment

Rotating tank with flat bottom and adjustable speed, dye such as $KMnO_4$ crystals.

Experiment

Fill tank with water and bring it to solid-body rotation. Drop dye crystals here and there. Allow for the dye to reach the bottom. Then reduce slightly the rotation rate and observe the transverse flow of dye very near the bottom. Increase slightly the rotation rate and observe a transverse flow in the opposite direction.

Notes

At typical rotation speeds in the laboratory, the molecular viscosity of water gives rise to extremely thin Ekman layers ($d = 0.6$ mm for $\nu = 1.01 \times 10^{-6}$ m^2/s and $\Omega = 30$ rpm). Consequently, the spiraling of the velocity vector can hardly be noticed. Use of glycerin ($\nu = 1.18 \times 10^{-3}$ m^2/s) yields thicker Ekman layers ($d = 2$ cm) and allows the spiraling effect to be seen by inspection from the side.

An inexpensive and convenient substitute for dye crystals is used coffee grounds.

Vagn Walfrid Ekman

1874 – 1954

Born in Sweden, V. W. Ekman spent his formative years under the tutelage of Vilhelm Bjerknes and Fridtjof Nansen in Norway. One day, Nansen asked Bjerknes to let one of his students make a theoretical study of the influence of the earth's rotation on wind-driven currents, on the basis of Nansen's observations during his polar expedition that ice drifts with ocean currents to the right of the wind. Ekman was chosen and later presented a solution in his doctoral thesis of 1902. As professor of mechanics and mathematical physics at the University of Lund in Sweden, Ekman became the most famous oceanographer of his generation. The distinguished theoretician also proved to be a skilled experimentalist. He designed a current meter and a reversing water bottle, which bear his name and which have been used extensively. Ekman was also the one who explained the phenomenon of dead waters by a celebrated laboratory experiment (see Figure 1-3). (*Photo courtesy of Pierre Welander.*)